

Inverse problems: Can we obtain more? Quantum dynamics and the ^4He case

E. Vitali, M. Rossi, L. Reatto, and D.E. Galli

Dipartimento di Fisica, Università degli Studi di Milano, via Celoria 16, 20133 Milano, Italy

(Dated: February 10, 2019)

We introduce a new strategy, called Genetic Inversion via Falsification of Theories (GIFT), to face inverse problems and we apply it to the extraction of information about real time dynamics of a many-body quantum system from noisy imaginary time correlation functions $f(\tau)$ computed via Quantum Monte Carlo (QMC). Production and falsification of model spectral functions $s(\omega)$ are obtained via a survival-to-compatibility with $f(\tau)$ evolutionary process, based on Genetic Algorithms. Statistical uncertainty in $f(\tau)$ is promoted to be an asset via a sampling of equivalent $f(\tau)$ within the noise, which give rise to independent evolutionary processes. We have studied bulk ^4He at $T = 0$ K; for the first time we recover from exact QMC simulations sharp quasi-particle excitations with spectral functions displaying also the multiphonon branch. We have studied the impuriton branch of one ^3He atom in liquid ^4He . We also studied vacancy-waves excitations in hcp solid ^4He finding a novel roton like feature.

PACS numbers: 02.30.Zz; 67.40.Db; 67.55.Jd; 67.55.Lf; 67.80.-s

I. INTRODUCTION

Since the earliest days of research in Physics, a deep question naturally arose: when building up a *theory*, how many answers may we expect from experimental *observations*? A theory has to predict the results of observations, but are we allowed to *deduce* a theory from them? This last question defines what is generally called an *inverse problem*, examples of which appear in a huge variety of physical or even more generally scientific studies^{1,2}. At a first glance, one feels that such an inverse procedure in realistic situations is unavoidably ill-posed, since any set of observations is limited and noisy, thus ruling out the possibility of finding out one and only one theory whose predictions fit such data. Following Popper³, in ref.⁴ the proposition was put forward that observations may only *falsify* a theory. In order to understand what does this mean in the realm of inverse problems, let's somehow formalize a typical situation. Consider the infinite abstract space \mathcal{S} containing all the possible theories describing a phenomenon, and a given set of observed data d concerning the same phenomenon. We may think d as an element of a space \mathcal{D} , containing all the possible results of ipothetical infinite measurements performed. The inverse problem would sound: may we find a theory $s \in \mathcal{S}$ predicting \mathcal{D} ? That is, can we find $s \in \mathcal{S}$ which is *not falsified* by any of the elements of \mathcal{D} ? But this is an idealized situation, since in a finite time we actually never know \mathcal{D} but only a subset $\mathcal{D}^* \subset \mathcal{D}$ whose elements are in general used to give an estimation of the statistical uncertainties in the observations. Normally an infinite number of theories exists compatible with \mathcal{D}^* ; it is then clear that we may exclude some theories but we still remain with a set $\mathcal{S}_{\mathcal{D}^*} \subset \mathcal{S}$ of equivalent “solutions”. Depending on the mathematical details of the space \mathcal{S} , a natural idea appears to be that of devising a procedure allowing to capture what do the theories in $\mathcal{S}_{\mathcal{D}^*}$ have in common. In this way, even if we won't succeed in finding out a unique theory $s \in \mathcal{S}$, we will be able nevertheless to

find out a class of features, providing physical properties, that s has to possess so that it will not be falsified by the limited set of observations.

II. INVERSE PROBLEMS AND QUANTUM DYNAMICS

We focus now on one particular inverse problem: the estimation of spectral functions of many-body quantum systems starting from imaginary time correlation functions computed in Quantum Monte Carlo (QMC) simulations. Indeed, the study of dynamical properties requires the evaluation of spectral functions $s(\omega)$:

$$s(\omega) = \int_{-\infty}^{+\infty} \frac{dt}{2\pi} e^{i\omega t} \langle e^{i\hat{H}t} \hat{A} e^{-i\hat{H}t} \hat{B} \rangle, \quad (1)$$

\hat{A} and \hat{B} being given operators acting on the Hilbert space of the system whose Hamiltonian operator is \hat{H} . The brackets indicate expectation value on the ground state or thermal average. Unfortunately, general methods to obtain exact real time evolution are not known, thus forcing us to *deduce a theoretical* $s(\omega)$ from “*observations*” of imaginary time correlation function $f(\tau) = \langle e^{\hat{H}\tau} \hat{A} e^{-\hat{H}\tau} \hat{B} \rangle$ which can be computed by QMC methods. The scenario is that of an inverse problem with the formal appearance of an integral equation

$$f(\tau) = \int_{-\infty}^{+\infty} d\omega \mathcal{K}(\tau, \omega) s(\omega) \quad (2)$$

where for example, at zero temperature, $\mathcal{K}(\tau, \omega) = \theta(\omega) e^{-\tau\omega}$, $\theta(\omega)$ being the Heaviside distribution. The difficulty lies in the fact that the kernel $\mathcal{K}(\tau, \omega)$ is a smoothing operator and QMC techniques are based on a discretization of the imaginary time domain, with time step $\delta\tau$, allowing an estimation of $f(\tau)$ only in correspondence with a finite number of imaginary time values

$\{0, \delta\tau, 2\delta\tau, \dots, l\delta\tau\}$, $\mathcal{F} \equiv \{f_0, f_1, \dots, f_l\}$; in general \mathcal{F} is obtained as an average of several QMC calculations of $f(\tau)$, each affected by statistical noise and which are used to estimate the *statistical uncertainties* $\{\sigma_0, \sigma_1, \dots, \sigma_l\}$ associated with \mathcal{F} . The task is then to evaluate $s(\omega)$ starting from limited and noisy data. Often sum rules provide useful help, either imposing exact constraints on $s(\omega)$ or allowing to perform additional QMC measurements which provide estimations for some momenta of $s(\omega)$: $\mathcal{C} \equiv \{c_n = \int_{-\infty}^{+\infty} d\omega \omega^n s(\omega), n \in \mathbb{Z}\}$ (for example $c_0 = \langle \hat{A}\hat{B} \rangle$ may be easily estimated in equilibrium QMC simulations with an associated statistical uncertainty). Moreover some *a priori knowledge* may be assumed such as the support, non-negativity or some further properties.

III. GENETIC INVERSION STRATEGY

The task of facing the problem in equation (2), namely an analytic continuation problem, has already been investigated: the Maximum Entropy Method⁵ (MEM) is the most widely popular strategy developed; in the realm of bulk quantum fluids it has provided only qualitatively interesting results^{6,7}. Another method has been proposed, the Average Spectrum Method⁸ (ASM), which has been recently applied to lattice spin models⁹. The ASM strategy, from our point of view, somehow captures the idea of extracting physical properties compatible with observations: an average between models is obtained by sampling a Bayesian probability distribution with a Metropolis algorithm. Here we want to follow more radically the general scheme outlined in the introduction: we need a space of models \mathcal{S} , containing a wide collection of spectral functions consistent with any *prior knowledge* about $s(\omega)$, a falsification procedure relying on the QMC “measurements” $d = \{\mathcal{F}, \mathcal{C}\}$ and a strategy to capture the accessible physical properties of $s(\omega)$. In our mathematical framework \mathcal{S} is made of step functions, providing a compromise between the possibility of suitably approximating *any* model of spectral function and the feasibility of numerical operations inside it. In the typical case ($\hat{A} = \hat{B}^\dagger$) when $s(\omega)$ is known to be real-valued, non-negative and the zero-momentum sum-rule holds, we rely on models \bar{s} of the form:

$$\bar{s}(\omega) = \sum_{j=0}^{m-1} \frac{s_j}{\mathcal{M}\Delta\omega} \chi_{A_j}(\omega), \quad \sum_{j=0}^{m-1} s_j = \mathcal{M} \quad . \quad (3)$$

$\bar{s}(\omega)$ differs from the physical spectral functions by a factor c_0 , the zero-momentum, which belongs to the set of observations and its role will become evident below. We introduce a discretization of the codomain, $s_j \in \mathbb{N} \cup \{0\}$, to make the space finite, and we use the characteristic function $\chi_{A_j}(\omega)$ of the intervals $A_j = [\omega_j, \omega_{j+1})$, $\{\omega_0, \dots, \omega_m\}$ being a partition of width $\Delta\omega$ of an interval of the real line larger than the hypothesized support of $s(\omega)$. \mathcal{M} provides the maximum number of quanta of spectral

weight available for the ensemble of the intervals A_j . How can we explore \mathcal{S} and falsify its elements? Genetic algorithms (GA) provide an extremely efficient tool to explore a sample space by a non-local stochastic dynamics, via a survival-to-fitness evolutionary process mimicking the natural selection we observe in natural world; such evolution aims towards “good” *building blocks*¹⁰ which, in our case, should recover information on physical spectral functions. The fitness of one particular $\bar{s}(\omega)$ should be based on the observations, i.e., on the noisy measured set d . But of course, taking into account the estimated statistical noise of d , any set d^* compatible with d provides equivalent information to build a fitness function. Thus in our GA any random set $d^* = \{\mathcal{F}^*, \mathcal{C}^*\}$ obtained by sampling independent Gaussian distributions centered on the original observations d , with variances which correspond to the estimated statistical uncertainties, can be used to define the fitness:

$$\Phi_{d^*}(\bar{s}) = -\alpha \sum_{j=0}^l \left[f_j^* - \int d\omega e^{-\omega j \delta\tau} c_0^* \bar{s}(\omega) \right]^2 - \sum_n \gamma_n \left[c_n^* - \int d\omega \omega^n c_0^* \bar{s}(\omega) \right]^2 \quad (4)$$

where the free parameters $\alpha, \gamma_n > 0$ are adjusted in order to make the contributions to Φ_{d^*} coming from \mathcal{F}^* and from \mathcal{C}^* of the same order of magnitude. If it happens that one c_n is exactly known, no error is added making $c_n^* = c_n$. In our GA, we start randomly constructing a collection of $\bar{s}(\omega)$; each $\bar{s}(\omega)$ is coded by m integers, s_j in equation (3). The genetic dynamics then consists in a succession of *generations* during which an initial *population*, consisting of $\mathcal{N}_{\bar{s}}$ *individuals*, is replaced with new ones in order to reach regions of \mathcal{S} where high values of the *fitness* exist, for a given d^* . In the passage between two generations a succession of “biological-like” processes take place: namely *selection*, *crossover* and *mutation*, which are operators acting on \mathcal{S} devised in such a way to comply with the definition in equation (3).

In our context the GA dynamics performs the falsification procedure: only the $\bar{s}(\omega)$ with the highest fitness in the last generation provides a model for $s(\omega)$ which has not been falsified by d^* . Many independent evolutionary processes may be generated by sampling different d^* , thus obtaining the set $\mathcal{S}_{\mathcal{D}^*}$ made of the elements $c_0^* \bar{s}(\omega)$; at this point an averaging procedure inside $\mathcal{S}_{\mathcal{D}^*}$ appears as the most natural way to extract physical informations. GIFT provides a more faithful implementation of the scheme described in the introduction than the ASM, where a falsification procedure is only partially obtained, exploring high probability model-space regions via a local Metropolis random walk, and where the statistical uncertainties in the observations play a marginal role, appearing only in the definition of the probability.

We have performed several tests on exactly solvable analytical models suitably discretized and “dirtyed” with random noise to “simulate” actual data. Having in mind

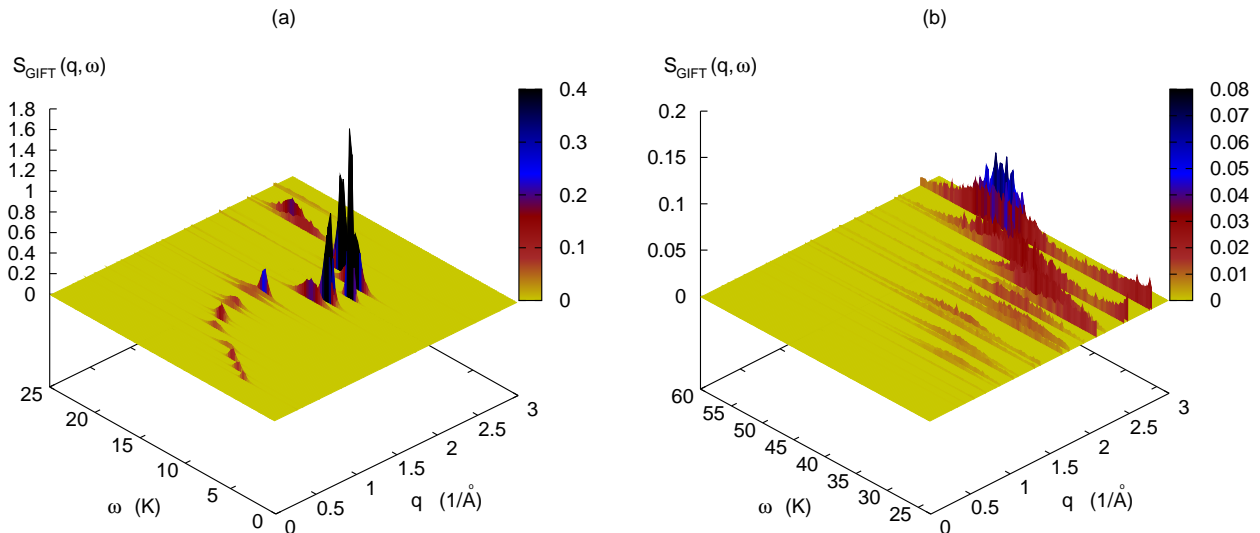


Figure 1: **Dynamical structure factor of superfluid ${}^4\text{He}$.** $S_{GIFT}(q, \omega)$ extracted at $\rho = 0.0218 \text{ \AA}^{-3}$ in the energy region of the quasi-particle peaks (a) and in the multiphonon region (b), for a discrete set of wave vectors compatible with the periodic boundary conditions used in the simulations with $N = 64, 128, 256$ ${}^4\text{He}$ atoms in a cubic box. Color scale represents bins' height.

the ${}^4\text{He}$ case, we have tried to reconstruct spectral functions consisting of linear combinations of gaussians, one sharp “peak” at small ω and one broad contribution at higher ω . We have observed that only some features of the exact solution can be consistently reproduced: We have no possibility to reconstruct exactly the shape of $s(\omega)$; on the other hand, access is granted to the identification of the presence of a sharp peak and to its position, to the position of the broad contribution, to some integral properties involving $s(\omega)$ and to its support.

IV. THE DYNAMICAL STRUCTURE FACTOR OF SUPERFLUID ${}^4\text{HE}$

We present now some applications of this approach; our first case study is the determination of the dynamical structure factor $S(q, \omega)$ of liquid bulk ${}^4\text{He}$. We have used the exact SPIGS method^{11,12} to compute the intermediate scattering function $F(q, \tau)$ at $T = 0$ K near the equilibrium density, $\rho = 0.0218 \text{ \AA}^{-3}$, and slightly above the freezing density, $\rho = 0.0262 \text{ \AA}^{-3}$; $F(q, \tau)$ is simply $f(\tau)$ when $\hat{A} = \hat{B}^\dagger$ is chosen to be the Fourier transform of the local density operator $\hat{A} = \hat{\rho}_{\vec{q}} = \sum_{i=1}^N e^{-i\vec{q}\cdot\vec{r}_i}$. We observe that our reconstructed $S_{GIFT}(q, \omega)$ exhibits an overall structure in good agreement with experimental data: a sharp quasi-particle peak and a shallow multiphonon maximum are present (see Fig.1). Both features appear for the first time within an analytic continuation

procedure applied to a QMC study of a many-body system in the continuum. In Fig.2 we show one $S_{GIFT}(q, \omega)$ in the roton region together with the excitation energies $\varepsilon(q)$ i.e., the position of the main peak as function of q . The uncertainties of $\varepsilon(q)$ correspond to the widths of the peaks σ_ε : we have checked the consistency of such identification by performing independent QMC estimations of $F(q, \tau)$ and comparing the positions of the peaks obtained in $S_{GIFT}(q, \omega)$; the distribution of the peaks displays a variance comparable to σ_ε^2 .

By integrating $S_{GIFT}(q, \omega)$ we have access to quantities like the strength of the single quasi-particle peak, $Z(q)$, and thus also to the contribution to the static structure factor, $S(q)$, coming from multiphonon excitations. Remarkably, $Z(q)$ turns out to be in close agreement with experimental data (see upper Fig.3), thus strongly suggesting that the shallow maximum in $S_{GIFT}(q, \omega)$ at large energy carries indeed reliable physical information on the multiphonon branch of the spectrum. The position of such multiphonon maximum (see Fig.2c) is in qualitative agreement with experiments¹³: as we have pointed out before, there is no possibility to recover the detailed shape of the spectral function within the present implementation of the GIFT method like the multiphonon substructures given by high resolution measurements¹⁵ of $S(q, \omega)$. In the lower panel of Fig.3 we show the static density response function $\chi(q)$ obtained evaluating the c_{-1} from $S_{GIFT}(q, \omega)$; the agreement with experiments is impressive, also near freezing¹⁶.

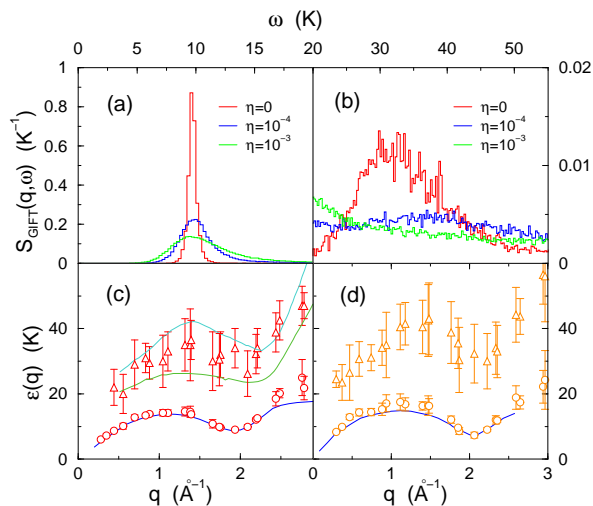


Figure 2: **Low energy excitations in superfluid ^4He .** $S_{GIFT}(q, \omega)$ at $q = 1.755 \text{ \AA}^{-1}$ and $\rho = 0.0218 \text{ \AA}^{-3}$; (a) single quasi-particle (qp) peak; (b) multiphonon (mp) contribution (notice change of scale). Lines corresponding to a $S_{GIFT}(q, \omega)$ obtained with a nonzero entropic prior ($\eta \neq 0$) are also shown. (c) $\varepsilon(q)$ extracted at $\rho = 0.0218 \text{ \AA}^{-3}$ from the position of the qp (circles) peaks and the positions of the maxima of the mp contribution (triangles) are shown. The error-bars represent the 1/2-height widths. (d) $\varepsilon(q)$ and mp contribution extracted at $\rho = 0.0262 \text{ \AA}^{-3}$. Lines in (c) and (d): experimental data^{13,14}; in the mp region in (c) the lower curve (green) represents the position of the maximum while the upper one (cyan) represents the 1/2-height width.

The calculation of the excitation spectrum $\varepsilon(q)$ in superfluid ^4He via QMC was addressed for instance in ref.17 and in ref.18, but here we are clearly much more ambitious because we aim to construct the full spectral function. Our method is so powerful that it is able to reveal the effects of even fine details of the interatomic interaction. For example, the computed spectrum $\varepsilon(q)$ in the phonon region is about 0.7 K above the experimental value. We understand this as an effect of truncation of the inter-atomic interaction $v(r)$ at a certain distance r_c . In most of our computations the interatomic potential is cut-off and displaced to zero at $r_c = 6 \text{ \AA}$, and the equation of state gives rise to an overestimation of the sound velocity by about 16%. We have performed some computations with $r_c = 14 \text{ \AA}$, in a simulation of $N = 512$ ^4He atoms and in this case the sound velocity turns out to be correct and now the theoretical $\varepsilon(q)$ at small q agrees with experiment within the resolution $\Delta\omega$. At $\rho = 0.0218 \text{ \AA}^{-3}$ we extract a roton energy of $E_R = 9.0 \pm 0.25 \text{ K}$ with the $v(r)$ in ref.19 and of $E_R = 8.5 \pm 0.5 \text{ K}$ with the $v(r)$ in ref.20, a potential considered more accurate (Experimental roton energy²¹ at SVP $E_R = 8.608 \pm 0.01 \text{ K}$). At $\rho = 0.0262 \text{ \AA}^{-3}$ we extract a roton energy of $E_R = 7.5 \pm 0.75 \text{ K}$ with the $v(r)$ in ref.19 and of $E_R = 7.6 \pm 0.35 \text{ K}$ with the $v(r)$ in ref.20 (Experimental roton energy²¹ at 24 bar $E_R = 7.3 \pm 0.02 \text{ K}$).

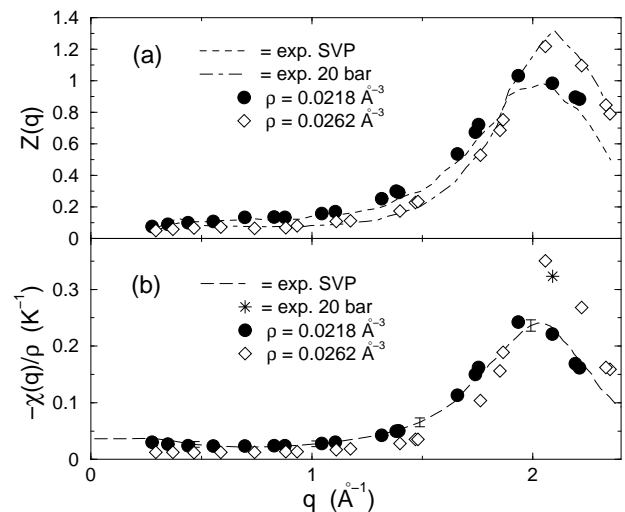


Figure 3: **Integrated quantities from spectral functions.** (a) GIFT strength of the quasi particle peak $Z(q)$ as function of q at two densities and experimental data¹⁵. (b) GIFT Static density response function $\chi(q)$ at two densities and experimental data^{13,16}. Error bars of theoretical results are smaller than the symbol size.

In order to compare GIFT results with those based on the strategy of MEM we have modified our fitness function by adding to Φ_{d^*} in equation (4) an entropic term $\eta S(\bar{s})$, S being the entropy as in ref.6 and η a free parameter, and using a constant as default model as in previous works^{6,7}. For all wave vectors \vec{q} we observed for the main peak of $S(q, \omega)$ a broadening (see Fig.2) strongly dependent on the choice of the parameter η . This implementation of MEM provides results comparable with those reported in references 6 and 7. The overall double-peak structure is always lost in presence of the entropic term: no sharp peak is present but only a smooth $S(q, \omega)$ survives, as function of ω , making the extracted excitation energy critically dependent on the value of η , thus introducing ambiguities in the interpretation of the results. In our original approach, i.e. without $\eta S(\bar{s})$, we have checked that none of the parameters (like \mathcal{M} , $\Delta\omega$, α , γ_n , ...) affects the class of features that we may trust to carry reliable physical information.

V. IMPURITY AND VACANCY DYNAMICS

Another interesting test case is provided by liquid ^4He in presence of one ^3He impurity, in order to extract the impurity branch which has been experimentally measured²². Variational results for such branch are known²³ but no results from exact QMC are available. This calculation requires the choice of $\hat{A} = e^{-i\vec{q}\cdot\vec{r}_{imp}}$, where \vec{r}_{imp} is the position of the impurity. In Fig.4 we show the reconstructed spectral functions together with the estimated dispersion relation obtained from a simulation of $N = 255$ ^4He atoms and one ^3He atom

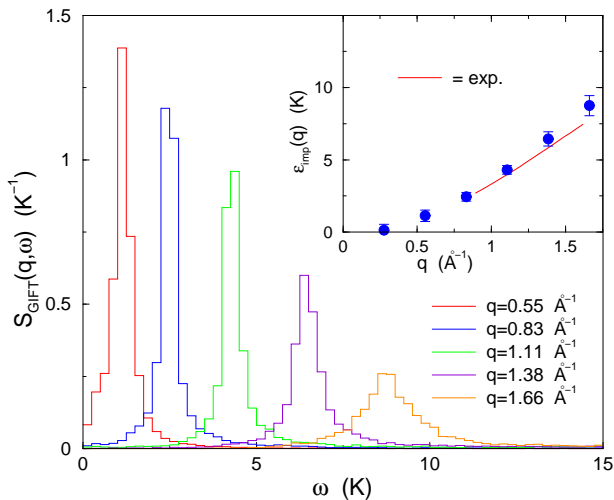


Figure 4: **^3He Impurity dynamics.** Impurity ^3He quasi-particle peak in superfluid ^4He at SVP for several wave vectors; in the inset the extracted excitation energies are shown together with experimental data²².

at $\rho = 0.0218 \text{ \AA}^{-3}$. The agreement with experimental data²² is very good, thus providing a robust check of validity of our approach.

As a further application of GIFT we have studied excitations in the solid phase, both longitudinal phonons and vacancy–waves. The results for longitudinal phonons will be presented elsewhere. In the present paper we will present only results for the excitation spectrum of a single vacancy in hcp solid ^4He at $\rho = 0.0293 \text{ \AA}^{-3}$, a density slightly above melting. The behaviour of vacancies in solid ^4He is of high interest because vacancies and other defects are believed to have a key role in the possible supersolid phase of ^4He at low temperature^{24,25}. In order to apply GIFT to vacancy dynamics the first step is the definition of a vector position \vec{x}_v that allows to follow the “motion” of the vacancy in imaginary time during a SPIGS simulation. This problem is much more difficult than the evaluation of the impurity branch, because the very definition of \vec{x}_v is far from trivial due to the large zero–point motion of the atoms in the low density solid. \vec{x}_v turns out to be a many–body variable, depending on all the vector positions of ^4He atoms, and even not free of ambiguities. We have employed two different procedures to obtain \vec{x}_v : the coarse-grain²⁷ and the Hungarian^{28,29}. In Fig.5 we show the vacancy excitation spectrum $\varepsilon_v(\vec{q})$ extracted from the vacancy spectral functions ($\hat{A} = e^{-i\vec{q}\cdot\vec{x}_v}$) obtained with the two methods. The results obtained with the two definitions of \vec{x}_v are very similar, and at first sight make evident a picture of Bloch waves in the crystal; the agreement with a tight binding hopping model³⁰ is good. Notice that $\varepsilon_v(\vec{q})$ represents the excitation energy with respect to the state with a vacancy with $|\vec{q}| = 0$, i.e., $\varepsilon_v(\vec{q})$ does not include the vacancy activation energy. By fitting $\varepsilon_v(\vec{q})$ with the tight binding expression

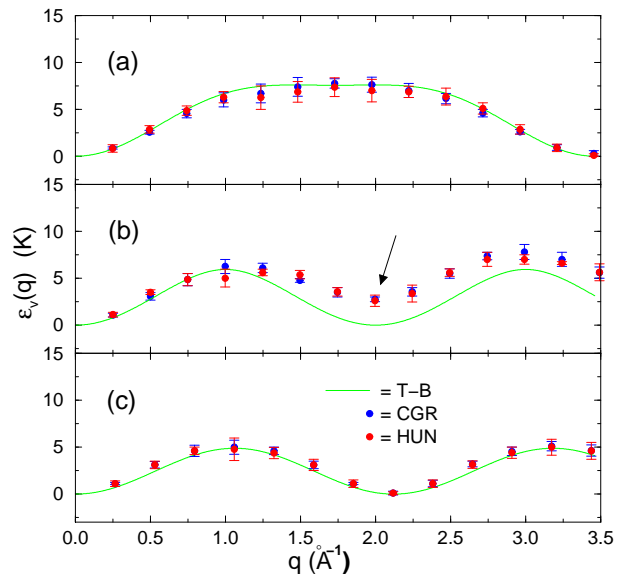


Figure 5: **Vacancy–waves dispersion relation in hcp solid ^4He .** Vacancy excitation spectrum in solid ^4He extracted from the $S_{GIFT}(q, \omega)$ of the vacancy–vector position \vec{x}_v at $\rho = 0.0293 \text{ \AA}^{-3}$ in a hcp lattice with $N=447$ particles along the principal symmetry directions: (a) ΓK , (b) ΓM and (c) ΓA . Two different algorithms have been used to obtain \vec{x}_v : a coarse-grain algorithm²⁷ (CGR) and the Hungarian algorithm^{28,29} (HUN). Dashed lines represent the spectrum of a tight binding model (T–B) for the hcp lattice³⁰ obtained imposing the values of the band width along the ΓK and ΓA directions equal to the average between the values extracted from the two different algorithms. The arrow points out the vacancy–roton mode.

we extract the vacancy effective mass in the different lattice directions: $m_{\Gamma K}^* = m_{\Gamma M}^* = 0.46 \pm 0.03 m_4$ and $m_{\Gamma A}^* = 0.55 \pm 0.1 m_4$, where m_4 is the ^4He mass; these values for m^* are in agreement with the results obtained with a different method in ref.31.

The agreement of $\varepsilon_v(\vec{q})$ with the tight binding model fails dramatically in the ΓM direction. In fact, at any reciprocal lattice vector the excitation energy should vanish. On the contrary at the first reciprocal lattice vector along ΓM the vacancy excitation spectrum does not vanish but it reveals a novel vacancy–roton mode with an energy of $2.6 \pm 0.4 \text{ K}$ and an effective mass of about $m_R^* = 0.46 m_4$. We have checked that this energy does not depend on the size of the system. Such behaviour of $\varepsilon_v(\vec{q})$ in the ΓM direction implies that the (non–zero) minimum is not a consequence of the lattice periodicity but it is related to correlated motion of particles like in superfluid ^4He . It is interesting that neutron scattering from hcp ^4He gives an unexpected excitation mode beyond the phonon modes exactly in the ΓM direction with a roton–like mode at the reciprocal wave vector²⁶. The experimental energy of such roton mode is about 4.4 times larger than what we find; so it is unclear the connection between our mode and experimental data. A

larger vacancy roton energy might arise in presence of clusters of vacancies. By analysing the contributions to $f(\tau) = \langle e^{\hat{H}\tau} \hat{A} e^{-\hat{H}\tau} \hat{A}^\dagger \rangle$ with $\hat{A} = e^{-i\vec{q}\cdot\vec{x}_v}$, one can see that the vacancy–roton mode is connected to motions of the vacancy between different basal planes. The fundamental difference between in–basal–plane and inter–basal–plane motions is that the lattice position in the first case is a centre of inversion whereas this is not so in the second case. The fact that hcp is not a Bravais lattice is fundamental in this respect. We have verified that in bcc crystal and in a two dimensional triangular lattice, both Bravais lattices, no such vacancy roton mode is present.

VI. CONCLUSIONS

We have built up a new strategy to attack inverse problems which has been used to study dynamics in quantum many–body systems from QMC simulations; we have obtained very accurate results in the ^4He case, in the liquid and in the solid phase, even in presence of disorder,

providing major improvements with respect to previous studies appeared in literature. We have stressed the important point that the problem we have faced belongs to the huge class of inverse problems, a deep topic also from a fundamental epistemologic³ point of view. The basic idea of the falsification principle⁴ guided us in our particular implementation of analytic continuation, but, of course, may provide important implications in many fields of scientific research. Moreover, every problem emerging in Physics or applied Mathematics that could be cast in the form of equation (2), independently of the specific kernel in equation (2), can be attacked with GIFT. The method can be extended to include different kinds of constraints on the spectral function or additional information like cross correlations between the statistical noise of $f(\tau)$ at different imaginary times. Many variants of GIFT can be devised depending on the problem, for instance a basis set different from step functions (3) can be used or non uniform discretization in presence of problems with multiple time scales, or distribution of noise that is not Gaussian.

-
- ¹ Päävāranta, L. & Somersalo, E. (Eds.) *Inverse Problems in Mathematical Physics* (Springer–Verlag Berlin, Heidelberg 1993).
- ² Kaipio, J. & Somersalo, E. *Statistical and Computational Inverse Problems* (Springer–Verlag, New York 2004).
- ³ Popper, K. *The Logic of Scientific Discovery* (Basic Books, 1959).
- ⁴ Tarantola, A. *Nature Physics* **2**, 492–494 (2006).
- ⁵ Jarrel, M. & Gubernatis, J.E. *Bayesian inference and the analytic continuation of imaginary–time quantum Monte Carlo data*. *Phys. Rep.* **269**, 133–195 (1996).
- ⁶ Boninsegni, M. and Ceperley, D.M. *Density fluctuations in liquid ^4He . Path Integrals and maximum entropy*. *J. Low Temp. Phys.* **104**, 339–357 (1996).
- ⁷ Baroni, S. & Moroni, S. *Reptation quantum Monte Carlo: a method for unbiased ground–state averages and imaginary–time correlations*. *Phys. Rev. Lett.*, **82**, 4745–4748 (1999).
- ⁸ White, S.R. *Computer Simulation Studies in Condensed Matter Physics III* 145–153 (Springer–Verlag Berlin, Heidelberg 1991).
- ⁹ Syljuåsen, O.F. *Using the average spectrum method to extract dynamics from quantum Monte Carlo simulations*. *Phys. Rev. B* **78**, 174429 1–10 (2008).
- ¹⁰ Goldberg, D.E. *Genetic Algorithms in Search, Optimization, and Machine Learning* (Addison–Wesley, 1989).
- ¹¹ Galli, D.E. & Reatto, L. *Recent progress in simulation of the ground state of many Boson systems*. *Mol. Phys.* **101**, 1697–1703 (2003).
- ¹² Galli, D.E. & Reatto, L. *The shadow path integral ground state method: study of confined solid ^4He* . *J. Low Temp. Phys.* **136**, 343–359 (2004).
- ¹³ Cowley, R.A. & Woods, A.D.B. *Inelastic scattering of thermal neutrons from liquid helium*. *Can. J. Phys.* **49**, 177–200 (1971).
- ¹⁴ Woods, A.D.B. & Cowley, R.A. *Structure and excitations of liquid helium*. *Rep. Prog. Phys.* **36**, 1135–1231 (1973).
- ¹⁵ Gibbs, M.R. Andersen, K.H. Stirling, W.G. & Schober, H. *The collective excitations of normal and superfluid ^4He : the dependence on pressure and temperature*. *J. Phys.: Condens. Matter* **11**, 603–628 (1999).
- ¹⁶ Caupin, F. Boronat, J. & Andersen, K.H. *Static structure factor and static response function of superfluid helium 4: a comparative analysis*. *J. Low Temp. Phys.* **152**, 108–121 (2008).
- ¹⁷ Moroni, S. Galli, D.E., Fantoni, S. & Reatto, L. *Variational theory of bulk ^4He with shadow wave functions: ground state and the phonon–maxon–roton spectrum*. *Phys. Rev. B* **58**, 909–924 (1998).
- ¹⁸ Boronat, J. & Casulleras, J. *Diffusion Monte Carlo for excited states: phonon and rotons in superfluid ^4He* . *J. Low Temp. Phys.* **110**, 443–448 (2008).
- ¹⁹ Aziz, R.A. Nain, V.P.S. Carley, J.S. Taylor, W.L. & McConville, G.T. *An accurate intermolecular potential for helium*. *J. Chem. Phys.* **70**, 4330–4342 (1979).
- ²⁰ Aziz, R.A. Janzen, A.R. Moldover, M.R. *Ab initio calculations for helium: a standard for transport property measurements* *Phys. Rev. Lett.* **74**, 1586–1589 (1995).
- ²¹ Stirling, W.G. *Excitations in Two–Dimensional and Three–Dimensional Quantum Fluids* 25–46 (Plenum Press, New York 1991).
- ²² Fåk, B. Guckelsberger, K. Körfer, Scherm, R. & Dianoux, A.J. *Elementary excitations in superfluid $^3\text{–}^4\text{He}$ mixtures: pressure and temperature dependence*. *Phys. Rev. B*, **41**, 8732–8748 (1990).
- ²³ Galli, D.E. Masserini, G.L. & Reatto, L. *Variational calculation of excited–state properties of a ^3He impurity in superfluid ^4He* . *Phys. Rev. B* **60**, 3476–3484 (1999).
- ²⁴ Kim, E. & Chan, M.H.W. *Probable observation of a super–solid helium phase*. *Nature* **427**, 225–227 (2004).

- ²⁵ Kim, E. & Chan, M.H.W. *Observation of superflow in solid helium*. *Science* **305**, 1941–1944 (2004).
- ²⁶ Blackburn, E. et al. *Neutron scattering study of the excitation spectrum of solid helium at ultra-low temperatures*. *PRAMANA–J. Phys.* **71**, 673–678 (2008).
- ²⁷ Prokof'ev, N. & Svistunov, B. *Supersolid state of matter*. *Phys. Rev. Lett.* **94**, 155302 1–4 (2005).
- ²⁸ Clark, B.K. & Ceperley, D.M. *Path Integral calculations of vacancies in solid helium* *Com. Phys. Comm* **179**, 82–88 (2008).
- ²⁹ Burkard, R.E. & Derigs, U. *Assignment and Matching Problems* (Springer-Verlag, Berlin, 1980).
- ³⁰ Galli, D.E. & Reatto, L. *Vacancy excitation spectrum in solid ^4He and longitudinal phonons*. *Phys. Rev. Lett.* **90**, 175301 1–4 (2003).
- ³¹ Pollet, L, et al. *Local stress and superfluid properties of solid ^4He* . *Phys. Rev. Lett.* **101**, 097202 1–4 (2008).

VII. ACKNOWLEDGEMENTS

We acknowledge useful discussions with S. Moroni. This work was supported by the Supercomputing facilities of CILEA.